

Structure–Activity Relationship of Metabolic Sialic Acid Inhibitors and Labeling Reagents

Sam J. Moons,^{||} Emiel Rossing,^{||} Mathilde A. C. H. Janssen, Torben Heise, Christian Büll, Gosse J. Adema, and Thomas J. Boltje*



Cite This: *ACS Chem. Biol.* 2022, 17, 590–597



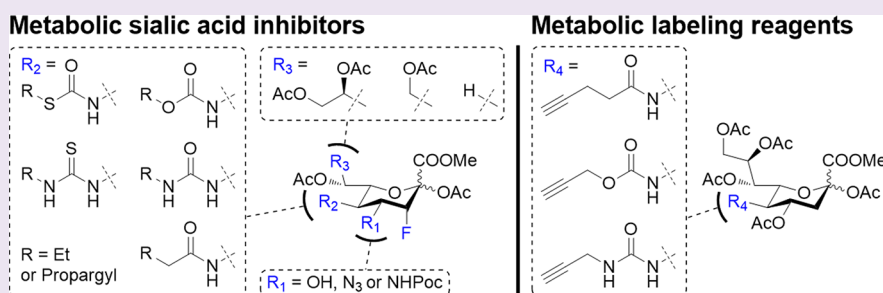
Read Online

ACCESS |

Metrics & More

Article Recommendations

Supporting Information



ABSTRACT: Sialic acids cap the glycans of cell surface glycoproteins and glycolipids. They are involved in a multitude of biological processes, and aberrant sialic acid expression is associated with several pathologies, such as cancer. Strategies to interfere with the sialic acid biosynthesis can potentially be used for anticancer therapy. One well-known class of sialylation inhibitors is peracetylated 3-fluorosialic acids. We synthesized 3-fluorosialic acid derivatives modified at the C-4, C-5, C-8, and C-9 position and tested their inhibitory potency *in vitro*. Modifications at C-5 lead to increased inhibition, compared to the natural acetamide at this position. These structure–activity relationships could also be applied to improve the efficiency of sialic acid metabolic labeling reagents by modification of the C-5 position. Hence, these results improve our understanding of the structure–activity relationships of sialic acid glycomimetics and their metabolic processing.

INTRODUCTION

Sialic acids are nine-carbon sugars abundantly expressed at the termini of mammalian glycans on membrane-bound and secreted glycoproteins and glycolipids. The sialic acid family contains >80 chemically distinct members that are related to the nonulosonic acids, nine-carbon backbone α -keto sugars that are widely found in nature.^{1,2} Mammalian cells can produce sialic acids *via* a *de novo* biosynthesis pathway starting from *N*-acetylmannosamine (ManNAc) in a three-step enzymatic process.³ Subsequently, sialic acids are converted into CMP-sialic acids by CMP-sialic acid synthase (CMAS). CMP-sialic acids are transported into the Golgi apparatus where they are utilized as a sialyl donor by 20 sialyltransferase isoenzymes which install sialic acids *via* distinct glycosidic linkages (α 2-3, α 2-6, or α 2-8) on various glycoconjugates (*N*/*O*-glycans, glycolipids) giving rise to so-called sialoglycans. Cell surface sialic acids are important modulators of a myriad of biological processes such as the binding and transport of ions, enhancing the viscosity of mucins, regulating glycoprotein half-life, and interacting with sialic acid binding proteins.⁴ Sialoglycans are recognized by sialic acid-binding immunoglobulin-like lectins (Siglecs), a family of immunoregulatory receptors,⁵ and selectins that mediate the trafficking of immune

cells. Sialic acids therefore play an important role in modulating immune activity.⁶

Cancers of various origins display altered cell surface glycosylation with the overexpression of sialic acid as a frequently observed feature. The overexpression of sialic acid in cancer arises from increased metabolic flux of the sialic acid pathway, increased sialyltransferase expression, and a decrease in sialidase expression. Cancer hypersialylation is associated with resistance to radio- and chemotherapy, apoptotic evasion, cancer progression, and metastasis and the induction of an immunosuppressive tumor microenvironment hence leading to aggressive and invasive forms of cancer with a poor prognosis.⁷ Blocking aberrant sialylation in cancer may therefore represent a promising therapeutic strategy.⁸ Bacterial sialidases have been investigated in clinical trials to reduce cancer sialylation albeit with limited success. Bacterial sialidases are often contaminated,^{9,10} immunogenic, and known to stay bound after

Received: November 5, 2021

Accepted: February 4, 2022

Published: February 18, 2022



the glycerol side chain led to erosion of inhibitory potency but interestingly could be recovered by also introducing C-5 modifications. The results demonstrate a clear structure–activity relationship for the metabolism of unnatural analogues resulting in more potent inhibitors than the P-SiaFNAC parent compound. Indeed, this guideline could be translated to also improve the efficacy of sialic acid metabolic labeling reagents (Figure 1). C-5 propargyl carbamates outperformed the corresponding thiourea and amide analogues resulting in more efficient metabolic labeling.

RESULTS AND DISCUSSION

Structure–Activity Relationship of Metabolic Sialic Acid Inhibitors. To enable the direct comparison of different C-5 derivatives, two sets of derivatives containing the same saturated [ethyl, 2, 4, 6, 8, 10, 12 (azidoethyl)] or unsaturated (propargyl, 3, 5, 7, 9, 11) chain length were prepared. Alkynes and azides are functional handles that can undergo orthogonal reactions in biological systems. We previously observed that the introduction of a heteroatom at C-5 (carbamate *vs* amide) led to increased metabolic processing by CMAS affording an increased intracellular concentration of the corresponding active CMP derivative.²⁰ Hence, we investigated various heteroatom substitution patterns in the form of C-5 amide (a)-, carbamate (oc)-, urea (ur)-, thiourea (tur)-, and *S*-thiocarbamate (tc)-containing compounds to establish their effect on the inhibitory potency.

P-SiaFNAC derivatives 2–12 were prepared from the corresponding C-5 amine by acylation in low to moderate yields of 7–44% (Scheme 1). Reactions at the C-5 amine in

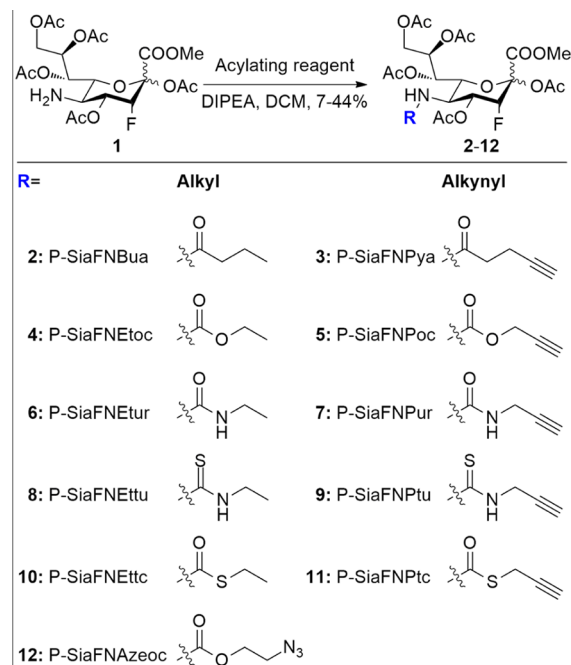
After 3 days, cellular sialylation was measured by staining for α 2-3-linked sialic acids using the MAL-II lectin. The EC₅₀ values were determined and defined as the concentration where a 50% decrease in lectin binding compared to the control (DMSO) was observed (Figure 2, Table 1).

All synthesized sialosides, with the exception of 3 and 11, are more potent inhibitors than P-SiaFNAC. This is in line with earlier research that showed that a carbamate group enabled increased metabolic processing by CMAS. Inhibitors having an *S*-thiocarbamate, urea, or thiourea linkage also show an increased inhibitor potency compared to P-SiaFNAC. For both series of compounds (ethyl and propargyl), a trend emerges with the carbamate and thiocarbamate linkage being the most potent, followed by the thiourea, then the urea, and the amide derivative being the least potent inhibitor. Propargyl thiocarbamate 11 showed toxicity at relatively low concentrations. To validate this trend, the potency of the inhibitors was also measured in a broader set of cell lines: Jurkat acute T-lymphocyte leukemia cells and murine EL-4 (T-lymphocyte leukemia), GL261 (glioma), and B16F10 (melanoma) cancer cell lines. As staining with MAL-II can lead to unwanted binding to 3-*O*-sulfated galactose residues,²⁷ we therefore switched to SNA-I, which binds α 2-6-linked sialic acid. Sialylation was measured at different concentrations of the inhibitors, and EC₅₀-values were calculated by fitting a dose–response curve and obtaining the concentration at which 50% of sialic acid remains on the cell surface.

For all cell lines, the new inhibitors also proved to be more potent than the parent compound P-SiaFNAC (Table 1). For several compounds, inhibition was found even in less-responsive murine cancer cell lines like EL-4. Although P-SiaFNAC shows low inhibitory potency (>50 μ M) in B16F10 cells *in vitro*, it has been shown to reduce tumor growth *in vivo*.¹⁴ Across the five cell lines, the observed trend in potency versus the type of C-5 modification is in line with observations for THP-1 cells, with compounds 4, 5, 10, and 12 being the most potent inhibitors. Next, we investigated the impact of modifications on the glycerol side chain of sialic acid (Scheme 2). Truncated octulosonic and heptulosonic acid inhibitors 16, 17, 20, and 21 were synthesized, containing either a 7- or 8-carbon skeleton. Additionally, C-5 carbamate derivatives were prepared to enable the comparison of these truncated inhibitors to the most potent carbamate inhibitor (4). We were also interested in probing to what extent modifications at the C-4 and glycerol side chain contributed to the activity of the sialyltransferase inhibitors. Hence, we prepared derivatives 23 and 25 having an azide or propargyloxycarbonyl at the C-4 position and a dual-modified inhibitor 24, which has a C-4 azide and C-5 carbamate.

Truncated derivatives 16, 17, 20, and 21 were synthesized from sialic acid glycol 13. Malaprade oxidation²⁸ followed by sodium borohydride reduction and acetylation afforded 14 and 18.²⁹ Selective N-deacetylation followed by acylation with ethyl chloroformate afforded carbamates 15 and 19. Electrophilic fluorination³⁰ and subsequent acetylation of acetamides 14 and 18 and carbamates 15 and 19 afforded truncated inhibitors 16, 17, 20, and 21. Subsequent fluorination and acetylation of 4-N₃-glucal 22³¹ afforded 23. In a similar manner as described above, selective N-deacetylation of 23 followed by acylation gave the C-4- and C-5-modified inhibitor 24. 25 was synthesized from 23 via a direct conversion of the azide to a propargyl carbamate.³²

Scheme 1. Synthesis of the SiaF Derivatives (2–12)



presence of a C-3 fluorine do not proceed efficiently presumably due to the lower amine nucleophilicity. The potency of the inhibitors 2–12 was tested on human THP-1 monocytic leukemia cells (Figure 2). Inhibitor potency was assessed by incubating cells with a range of inhibitor concentrations for 3 days to allow for sialoglycan turnover.

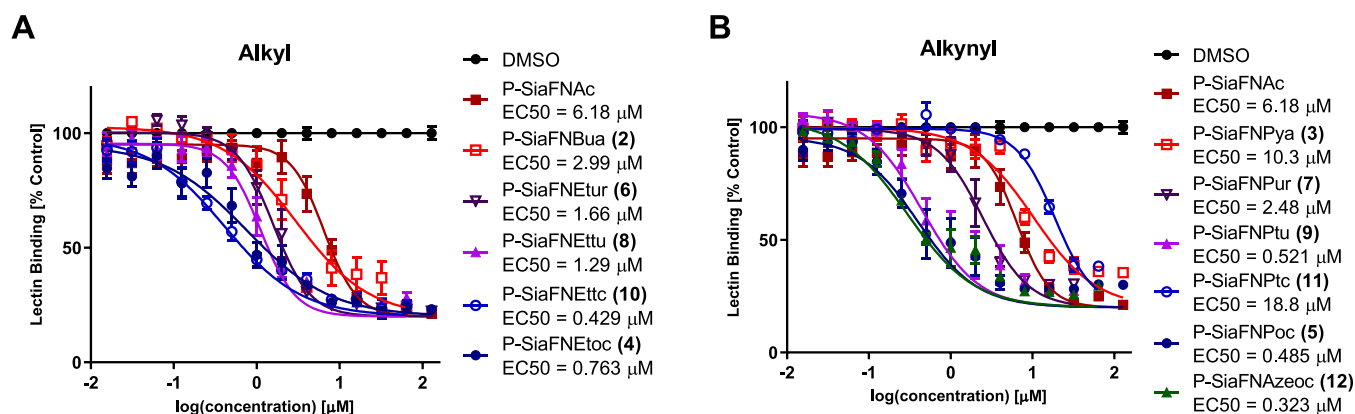


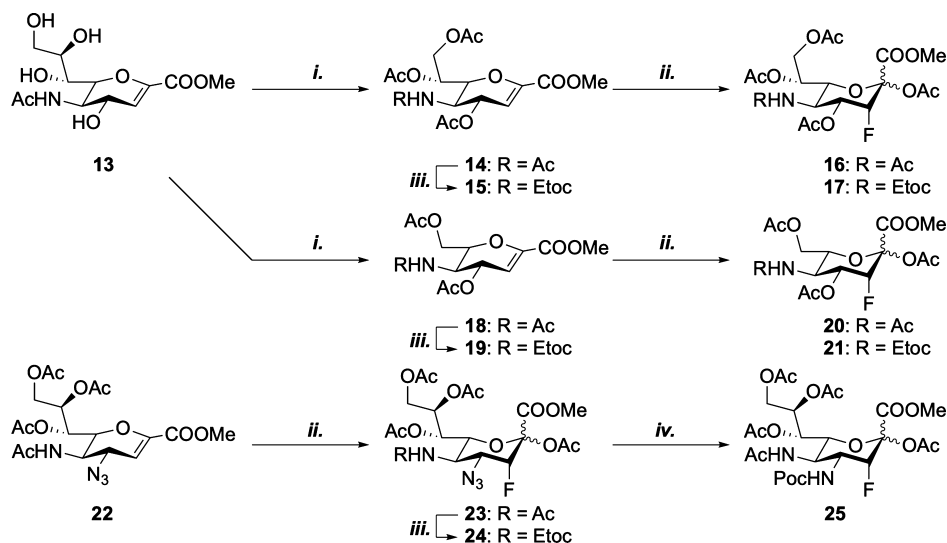
Figure 2. Dose-dependent inhibition of α -2-3-linked sialic acid by (A) alkyl-substituted and (B) alkynyl-substituted fluorinated sialic acid analogues. THP-1 cells were cultured for 3 days with 0–256 μ M fluorinated sialic acid analogues 2–12 and then stained with biotinylated MAL-II for α -2-3-linked sialic acid, followed by streptavidin–PE. Fluorescence was measured using flow cytometry and normalized to a DMSO control. Values are plotted as mean \pm standard error means.

Table 1. EC₅₀ Values in μ M for Inhibition of α -2-3-Linked Sialic Acid (First Column) and α -2-6-Linked Sialic Acid^a

side group	P-SiaFNR	THP-1 (MAL-II)	THP-1 (SNA-I)	Jurkat (SNA-I)	GL261 (SNA-I)	B16F10 (SNA-I)	EL-4 (SNA-I)
alkyl	Ac	6.18	6.78	9.46	71.3	110	\geq 250
	Bua (2)	2.99	1.63	2.46	9.71	16.5	212
	Etoc (4)	0.763	0.319	0.48	5.71	11.5	77.7
	Etm (6)	1.66	1.76	3.32	11.2	29.4	46.1
	Ettu (8)	1.29	0.749	2.01	11.2	36.2	\geq 250
	Ettc (10)	0.429	0.780	1.29	7.81	11.9	89.1
alkynyl	Pya (3)	10.3	3.72	13.8	58.9	16.5	\geq 250
	Poc (5)	0.485	0.199	1.00	4.40	7.10	119
	Pur (7)	2.48	3.45	9.21	11.1	37.0	\geq 250
	Ptu (9)	0.521	1.92	5.08	16.3	197	60.4
	Ptc(11) ^b	18.6 ^b	46.6 ^b	N.D.	N.D.	N.D.	N.D.
other	Azeoc (12)	0.323	0.410	2.95	5.11	8.89	141

^aCells were cultured for 3 days with 0–256 μ M fluorinated sialic acid analogues 2–12 and then stained with biotinylated SNA-I or MAL-II lectins, followed by streptavidin–PE. Fluorescence was measured using flow cytometry and normalized to a DMSO control. ^bAmbiguous fit, due to toxicity at >32 μ M.

Scheme 2. Synthesis of C-4-, C-7-, and C-8-Modified Sialic Acid Inhibitors; (i) (1) NaIO₄, MeOH; (2) NaBH₄, MeOH; (3) Ac₂O, Py, 37% (14); 66% (18); (ii) (1) Selectfluor, DMF, H₂O; (2) Ac₂O, Py, 21% (16); 23% (17); 33% (20); 14% (21); 54% (23); (iii) (1) Tf₂O, 2-FPy, DCM, then 1,2-Propanediol; (2) Ethyl Chloroformate, DIPEA, DCM, 68% (15); 39% (19); 28% (24); and (iv) PMe₃, THF, then Propargyl Chloroformate, 24% (25)



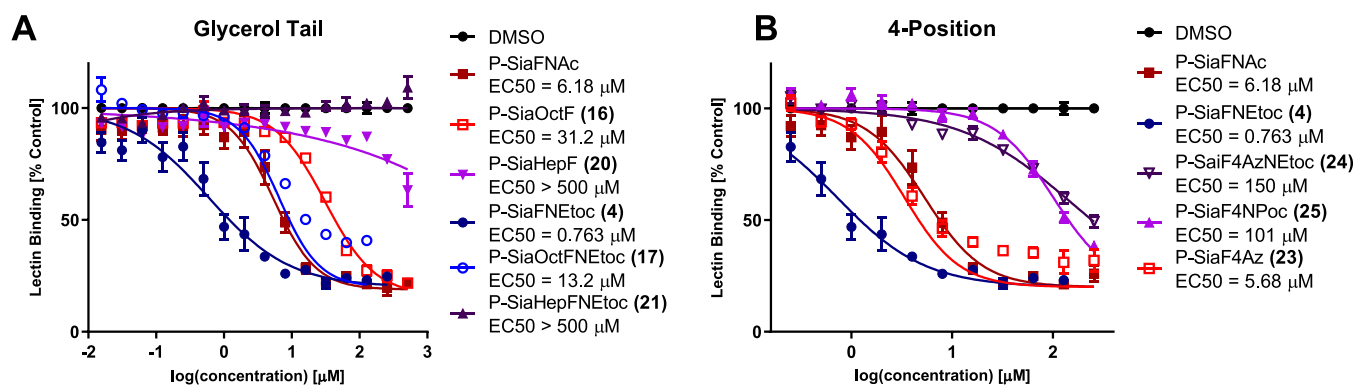


Figure 3. Dose-dependent inhibition of α 2-3-linked sialic acid by (A) truncated and (B) C-4-substituted fluorinated sialic acid analogues. Cells were cultured for 3 days with 0–512 μ M fluorinated sialic acid analogues 4, 16, 17, 20, 21, and 23–25 and stained with biotinylated MAL-II for α 2-3-linked sialic acid, followed by streptavidin–PE. Fluorescence was measured using flow cytometry and normalized to a DMSO control. Values are plotted as mean \pm standard error means.

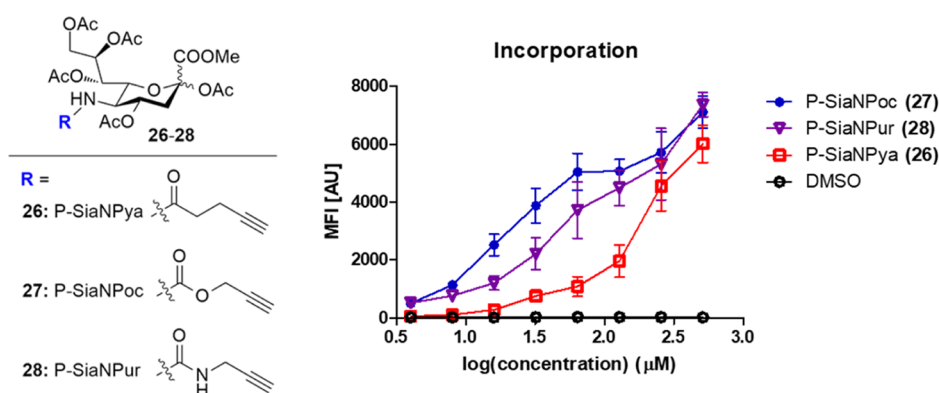


Figure 4. Incorporation of alkyne-containing sugars into cell surface glycans. THP-1 cells were cultured for 3 days with compounds (26–28) at concentrations of 4–512 μ M and DMSO as the negative control ($n = 3$). Incorporation was visualized using CuAAC, and fluorescence was measured using flow cytometry. Mean fluorescence was plotted against the logarithmic concentration as mean \pm standard error means.

Using the aforementioned protocol, the inhibitory potency of 16, 17, 20, 21, and 23–25 was tested on THP-1 cells (Figure 3). Truncation of the glycerol tail leads to a length-dependent decrease in inhibition. Octulosonic acid 16 shows a loss of activity compared to P-SiaFNAC. Interestingly, substitution of the C-5 acetamide for a carbamate leads to a recovery of inhibitory potency. Both heptulosonic acids 20 and 21 barely show any activity. The introduction of a C-4 azide (23) leads to comparable activity compared to P-SiaFNAC. Swapping the azide for a propargyl carbamate (25) led to a loss of activity, indicating that only small modifications at this position are tolerated. Remarkably, a C-5 carbamate in combination with a C-4 azide (24) leads to a notable reduction of the inhibitory potency in contrast to earlier research showing that carbamate inhibitors were more potent.²⁰

Structure–Activity Relationship of Metabolic Sialic Acid Labeling Reagents. From these results, it is clear that C-5 modification can be used to improve the efficiency of metabolic inhibitors. To investigate whether increased metabolic processing can also be employed to improve the metabolic labelling of sialic acids, three non-fluorinated alkyne-containing sialic acid derivatives (26–28) were prepared (see the Supporting Information). These derivatives carry the same alkyne reporter which is connected *via* a C-5 amide, urea, or carbamate group, analogous to compounds 3, 5, and 7 (Figure 4). THP-1 cells were incubated with 4–512 μ M 26–28 for 3

days. Incorporation was visualized by conjugating the incorporated alkyne to azide-biotin, followed by incubating with streptavidin, conjugated to a phycoerythrin dye (PE). Fluorescence was then measured with flow cytometry. As shown in Figure 4, carbamate 27 shows the most efficient incorporation, followed by urea 28 and amide 26. To minimize the impact of differences in alkyne reactivity in the biotin conjugation step, a large excess of the azide reagent was used to drive the reaction to completion. Furthermore, the use of high concentrations of the sialic acid derivative (26–28) leads to a similar plateau in the fluorescence signal, which would not be expected if differences in alkyne reactivity played a role. Moreover, the concentration-dependent incorporation of compounds 26–28 follows the same trend as the inhibitor analogues 3, 5, and 7.

CONCLUSIONS

We have prepared and tested a panel of C-4, C-5, C-7, and C-8 derivatives of (3-fluoro-)sialic acid. C-5 carbamate, urea, thiourea, and *S*-thiocarbamate derivatives are more potent inhibitors than the corresponding C-5 amides. Small modifications at the C-4 are tolerated, and adjustment of the glycerol side chain leads to a length-dependent decrease in inhibition. Incorporation of non-fluorinated analogues shows a similar trend with respect to the C-5 linkage as their fluorinated counterparts. These results could be considered

for further inhibitor design and for sialosides that utilize the same metabolic pathway.

METHODS

Cell Culture. THP-1 cells (TIB-202, ATCC) and Jurkat cells (TIB-152, ATCC) were cultured in RPMI-1640 medium containing 2 mM glutamine and 25 mM *N*-(2-hydroxyethyl)piperazine-*N'*-ethanesulfonic acid (Gibco, Life Technologies), supplemented with 10% v/v heat-inactivated fetal bovine serum (FBS) (Gibco, Life Technologies) and 1× antibiotic–antimycotic solution (100 units/mL penicillin, 100 µg/mL streptomycin, and 0.25 µg/mL Fungizone) (Gibco, Life Technologies) and passaged every 3–4 day by seeding a fraction of 0.5–2 mln cells of the culture per 10 mL medium.

EL-4 cells (TIB-39, ATCC) were cultured in Dulbecco's modified Eagle's medium (DMEM) (Gibco, Life Technologies), supplemented with 10% v/v heat-inactivated FBS (Gibco, Life Technologies), 1× antibiotic–antimycotic solution (100 units/mL penicillin, 100 µg/mL streptomycin, and 0.25 µg/mL Fungizone) (Gibco, Life Technologies), and 2 mM glutamine (Gibco, Life Technologies) and passaged every 2–4 days by seeding a fraction of 0.5–1 mln cells of the culture per 10 mL medium.

B16F10 cells (CRL-6475, ATCC) and GL261 cells were cultured in DMEM (Gibco), supplemented with 10% v/v heat-inactivated FBS (Gibco, Life Technologies), 1× antibiotic–antimycotic solution (100 units/mL penicillin, 100 µg/mL streptomycin, and 0.25 µg/mL Fungizone) (Gibco, Life Technologies), and 2 mM glutamine (Gibco, Life Technologies) and passaged every 2–4 days at 70–80% confluency. For passaging a T75 flask (Corning), medium was removed, and the monolayer was washed with 10 mL of phosphate-buffered saline (PBS) pH 7.2 without CaCl₂ and MgCl₂ (Gibco, Life Technologies) before adding 3.5 mL of 0.05% trypsin/EDTA solution (Gibco, Life Technologies) in PBS. Cells were incubated at room temperature for 30–45 s after which the trypsin/EDTA solution was removed. Cells were incubated for an additional 2 min at 37 °C and 5.0% CO₂ and resuspended in cell culture medium. Cells were then seeded at ~40,000 cells/cm² in new culture flasks.

Lectin Staining of Cells. The protocol mentioned below was repeated until $n \geq 3$ for each compound using cells at different passage numbers.

Cells were cultured in medium containing different concentrations of unnatural sugar derivatives on either a 48-well plate (adherent cell lines; 20,000–40,000 cells per well) (Corning) or a 96-well plate (suspension cell lines; 13,000–20,000 cells per well) (Thermo Scientific). DMSO, at same dilution as the unnatural sugar derivative stock solutions, was used as a positive control for lectin staining; P-SiaFNAC was used for all concentrations as the negative control. Cells were incubated for 3 days at 37 °C and 5% CO₂ in a humidified incubator.

Cells were harvested and washed with 100 µL of 1× CF-blocking buffer (Vector Laboratories Inc.) containing 1 mM CaCl₂ and 1 mM MgCl₂. The cells were then resuspended in 50 µL of 0.5 µg/mL 0.5 ng/mL biotinylated lectin in 1× carbo-free blocking buffer and incubated at 4–8 °C for 45–60 min. Cells were washed with 3 × 100 µL of PBA (PBS-containing 1% v/v FBS and 0.1% w/w NaN₃) and incubated with 40 µL of the 1 µg/mL streptavidin–phycoerythrin conjugate (Invitrogen, eBioscience) in PBA for 10–15 min at 4–8 °C. Cells were then washed again with 3 × 100 µL of PBA, resuspended in PBA, and fluorescence was measured with a flow cytometer (Beckman & Dickinson FACS-Calibur). Each replicate was obtained for each condition with >10,000 gated events. Data were processed using FlowJo (FlowJo LLC). The percentage of lectin binding was obtained by normalizing the MFI values to the MFI values of the respective DMSO control.

Lectin Specificity Assay. The protocol mentioned below was repeated until $n \geq 3$ for each compound using cells at different passage numbers.

Culture medium was prepared in 96-well plates (Thermo Scientific). For every unnatural sugar derivative, 11 wells containing 100 µM unnatural sugar derivatives and 11 wells containing 10 µM

the unnatural sugar derivatives were prepared. DMSO, at same dilution as the tested probes, was used as a positive control for lectin staining. THP-1 Cells were cultured in the plates (20,000 cells per well), and the cells were incubated for 3 days at 37 °C and 5% CO₂.

Cells were harvested and washed with 100 µL of 1× CF-blocking buffer (Vector Laboratories Inc.) containing 1 mM CaCl₂ and 1 mM MgCl₂. The cells were then resuspended in 50 µL of 0.5 µg/mL either 0.5 ng/mL biotinylated AAL, AOL, SNA, MAL-II, WGA, LCA, PSA, PNA, PHA-L, or GSL-1 lectin in 1× carbo-free blocking buffer or with 50 µL of non-supplemented 1× carbo-free blocking buffer and incubated at 4–8 °C for 45–60 min. Cells were washed with 3 × 100 µL of PBA (PBS containing 1% v/v FBS and 0.1% w/w NaN₃), incubated with 40 µL of the 1 µg/mL streptavidin–phycoerythrin conjugate (Invitrogen, eBioscience) in PBA for 10–15 min at 4–8 °C. Cells were then washed again with 3 × 100 µL of PBA, resuspended in PBA, and fluorescence was measured with a flow cytometer (Beckman & Dickinson FACS-Calibur). Each replicate was obtained for each condition with >10,000 gated events. Data were processed using FlowJo (FlowJo LLC). The percentage of lectin binding was obtained by normalizing the MFI values to the MFI values of the respective DMSO control.

CuAAC Staining of the Cell Membrane. The protocol mentioned below was repeated until $n \geq 3$ for each compound using cells at different passage numbers.

THP-1 cells were cultured in medium containing 4–512 µM unnatural sugar derivatives on 96-well plates (20,000 cells per well) (Thermo Scientific). DMSO, at the same dilution as the unnatural sugar derivative stock solutions, was used as the negative control. Cells were incubated for 3 days at 37 °C and 5% CO₂ in a humidified incubator.

Cells were harvested and washed with 100 µL of 2× PBS. The cells were then resuspended in 95 µL of reaction buffer [250 µM CuSO₄, 200 µM L-histidine, 100 µM of azide-PEG3-biotin conjugate (click chemistry tools) in PBS], and 5 µL of a freshly made solution of sodium ascorbate (10 mM in PBS, final concentration of 500 µM) was added, after which cells were incubated at 37 °C for 20 min. Cells were washed with 3 × 100 µL of PBS containing 1% w/v BSA without NaN₃ and incubated with 40 µL of the 1 µg/mL streptavidin–phycoerythrin conjugate (BD, Pharmingen) in PBA (PBS containing 1% w/v BSA with 0.2% w/v NaN₃) for 20 min at 4–8 °C. Cells were then washed again with 3 × 100 µL of PBA, resuspended in PBA, and fluorescence was measured using a flow cytometer (Beckman Coulter FACS-CyAn ADP). Each replicate was obtained for each condition with >10,000 gated events. Data were processed using FlowJo (FlowJo LLC) and Graphpad Prism v5.0.

ASSOCIATED CONTENT

Supporting Information

The Supporting Information is available free of charge at <https://pubs.acs.org/doi/10.1021/acscchembio.1c00868>.

Supplemental table, synthetic procedures, and characterization of new compounds (PDF)

AUTHOR INFORMATION

Corresponding Author

Thomas J. Boltje – Cluster of Molecular Chemistry, Institute for Molecules and Materials, Radboud University Nijmegen, Nijmegen 6525 AJ, The Netherlands; orcid.org/0000-0001-9141-8784; Email: thomas.boltje@ru.nl

Authors

Sam J. Moons – Cluster of Molecular Chemistry, Institute for Molecules and Materials, Radboud University Nijmegen, Nijmegen 6525 AJ, The Netherlands

Emiel Rossing – Cluster of Molecular Chemistry, Institute for Molecules and Materials, Radboud University Nijmegen, Nijmegen 6525 AJ, The Netherlands

Mathilde A. C. H. Janssen – Cluster of Molecular Chemistry, Institute for Molecules and Materials, Radboud University Nijmegen, Nijmegen 6525 AJ, The Netherlands

Torben Heise – Cluster of Molecular Chemistry, Institute for Molecules and Materials, Radboud University Nijmegen, Nijmegen 6525 AJ, The Netherlands

Christian Büll – Department of Biomolecular Chemistry, Institute for Molecules and Materials, Radboud University Nijmegen, Nijmegen 6525 GA, The Netherlands

Gosse J. Adema – Radiotherapy & OncoImmunology Laboratory, Department of Radiation Oncology, Radboud University Medical Center, Nijmegen 6525 GA, The Netherlands

Complete contact information is available at:

<https://pubs.acs.org/10.1021/acschembio.1c00868>

Author Contributions

[†]S.J.M. and E.R. contributed equally.

Notes

The authors declare the following competing financial interest(s): These molecules are patented by our university

ACKNOWLEDGMENTS

This work was supported by an ERC-Stg (GlycoEdit, 758913) awarded to T.J.B.

REFERENCES

- (1) Angata, T.; Varki, A. Chemical diversity in the sialic acids and related α -keto acids: an evolutionary perspective. *Chem. Rev.* **2002**, *102*, 439–470.
- (2) Schauer, R.; Kamerling, J. P. Exploration of the Sialic Acid World. In *Adv. Carbohydr. Chem. Biochem.*; Baker, D. C., Ed.; Academic Press, 2018; Chapter 1, pp 1–213.
- (3) Moons, S. J.; Adema, G. J.; Derks, M. T.; Boltje, T. J.; Büll, C. Sialic acid glycoengineering using N-acetylmannosamine and sialic acid analogs. *Glycobiology* **2019**, *29*, 433–445.
- (4) Varki, A.; Cummings, R. D.; Esko, J. D.; Stanley, P.; Hart, G. W.; Aebi, M.; Darvill, A. G.; Kinoshita, T.; Packer, N. H.; Prestegard, J. H. *Essentials of Glycobiology*; Cold Spring Harbor Laboratory Press, 2015.
- (5) Macauley, M. S.; Crocker, P. R.; Paulson, J. C. Siglec-mediated regulation of immune cell function in disease. *Nat. Rev. Immunol.* **2014**, *14*, 653–666.
- (6) Ley, K. The role of selectins in inflammation and disease. *Trends Mol. Med.* **2003**, *9*, 263–268.
- (7) Büll, C.; den Brok, M. H.; Adema, G. J. Sweet escape: sialic acids in tumor immune evasion. *Biochim. Biophys. Acta, Rev. Cancer* **2014**, *1846*, 238–246.
- (8) Smith, B. A. H.; Bertozzi, C. R. The clinical impact of glycobiology: targeting selectins, Siglecs and mammalian glycans. *Nat. Rev. Drug Discovery* **2021**, *20*, 217–243.
- (9) Crespo, H. J.; Guadalupe Cabral, M.; Teixeira, A. V.; Lau, J. T. Y.; Trindade, H.; Videira, P. A. Effect of sialic acid loss on dendritic cell maturation. *Immunology* **2009**, *128*, e621–e631.
- (10) Stamatou, N. M.; Curreli, S.; Zella, D.; Cross, A. S. Desialylation of glycoconjugates on the surface of monocytes activates the extracellular signal-related kinases ERK 1/2 and results in enhanced production of specific cytokines. *J. Leukocyte Biol.* **2004**, *75*, 307–313.
- (11) Sedlacek, H.; Seiler, F. Immunotherapy of neoplastic diseases with neuraminidase: Contradictions, new aspects, and revised concepts. *Cancer Immunol. Immunother.* **1978**, *5*, 153–163.
- (12) Moustafa, I.; Connaris, H.; Taylor, M.; Zaitsev, V.; Wilson, J. C.; Kiefel, M. J.; Von Itzstein, M.; Taylor, G. Sialic acid recognition by *Vibrio cholerae* neuraminidase. *J. Biol. Chem.* **2004**, *279*, 40819–40826.
- (13) Petitou, M.; Rosenfeld, C.; Sinay, P. A new assay for cell-bound neuraminidase. *Cancer Immunol. Immunother.* **1977**, *2*, 135–137.
- (14) Büll, C.; Boltje, T. J.; Wassink, M.; de Graaf, A. M.; van Delft, F. L.; den Brok, M. H.; Adema, G. J. Targeting aberrant sialylation in cancer cells using a fluorinated sialic acid analog impairs adhesion, migration, and in vivo tumor growth. *Mol. Cancer Ther.* **2013**, *12*, 1935–1946.
- (15) Cohen, M.; Elkabets, M.; Perlmutter, M.; Porgador, A.; Voronov, E.; Apte, R. N.; Lichtenstein, R. G. Sialylation of 3-methylcholanthrene-induced fibrosarcoma determines antitumor immune responses during immunoeediting. *J. Immunol.* **2010**, *185*, 5869–5878.
- (16) Gray, M. A.; Stanczak, M. A.; Mantuano, N. R.; Xiao, H.; Pijnenborg, J. F. A.; Malaker, S. A.; Miller, C. L.; Weidenbacher, P. A.; Tanzo, J. T.; Ahn, G.; Woods, E. C.; Läubli, H.; Bertozzi, C. R. Targeted glycan degradation potentiates the anticancer immune response in vivo. *Nat. Chem. Biol.* **2020**, *16*, 1376–1384.
- (17) Rillahan, C. D.; Antonopoulos, A.; Lefort, C. T.; Sonon, R.; Azadi, P.; Ley, K.; Dell, A.; Haslam, S. M.; Paulson, J. C. Global metabolic inhibitors of sialyl- and fucosyltransferases remodel the glycome. *Nat. Chem. Biol.* **2012**, *8*, 661–668.
- (18) Guo, C.-T.; Sun, X.-L.; Kanie, O.; Shortridge, K. F.; Suzuki, T.; Miyamoto, D.; Hidari, K. I.-P. J.; Wong, C.-H.; Suzuki, Y. An O-glycoside of sialic acid derivative that inhibits both hemagglutinin and sialidase activities of influenza viruses. *Glycobiology* **2002**, *12*, 183–190.
- (19) van Scherpenzeel, M.; Conte, F.; Bull, C.; Ashikov, A.; Hermans, E.; Willems, A.; van Tol, W.; Kragt, E.; Moret, E.; Heise, T. Dynamic analysis of sugar metabolism reveals the mechanisms of action of synthetic sugar analogs. *BioRxiv* **2020**, DOI: [10.1101/2020.09.15.288712](https://doi.org/10.1101/2020.09.15.288712).
- (20) Heise, T.; Pijnenborg, J. F. A.; Büll, C.; van Hilten, N.; Kers-Rebel, E. D.; Balneger, N.; Elferink, H.; Adema, G. J.; Boltje, T. J. Potent metabolic sialylation inhibitors based on C-5-modified fluorinated sialic acids. *J. Med. Chem.* **2018**, *62*, 1014–1021.
- (21) Büll, C.; Boltje, T. J.; Balneger, N.; Weischer, S. M.; Wassink, M.; van Gemst, J. J.; Bloemendal, V. R.; Boon, L.; van der Vlag, J.; Heise, T.; den Brok, M. H.; Adema, G. J. Sialic acid blockade suppresses tumor growth by enhancing T-cell-mediated tumor immunity. *Cancer Res.* **2018**, *78*, 3574–3588.
- (22) Büll, C.; Boltje, T. J.; van Dinther, E. A. W.; Peters, T.; de Graaf, A. M. A.; Leusen, J. H. W.; Kreutz, M.; Figdor, C. G.; den Brok, M. H.; Adema, G. J. Targeted delivery of a sialic acid-blocking glycomimetic to cancer cells inhibits metastatic spread. *ACS Nano* **2015**, *9*, 733–745.
- (23) Büll, C.; Collado-Camps, E.; Kers-Rebel, E. D.; Heise, T.; Sondergaard, J. N.; Den Brok, M. H.; Schulte, B. M.; Boltje, T. J.; Adema, G. J. Metabolic sialic acid blockade lowers the activation threshold of mDCs for TLR stimulation. *Immunol. Cell Biol.* **2017**, *95*, 408–415.
- (24) Edgar, L. J.; Thompson, A. J.; Vartabedian, V. F.; Kikuchi, C.; Woehl, J. L.; Teijaro, J. R.; Paulson, J. C. Sialic Acid Ligands of CD28 Suppress Costimulation of T Cells. *ACS Cent. Sci.* **2021**, *7*, 1508–1515.
- (25) Heise, T.; Langereis, J. D.; Rossing, E.; de Jonge, M. I.; Adema, G. J.; Büll, C.; Boltje, T. J. Selective inhibition of sialic acid-based molecular mimicry in *Haemophilus influenzae* abrogates serum resistance. *Cell Chem. Biol.* **2018**, *25*, 1279–1285.
- (26) Büll, C.; Heise, T.; Beurskens, D. M.; Riemersma, M.; Ashikov, A.; Rutjes, F. P.; van Kuppevelt, T. H.; Lefeber, D. J.; den Brok, M. H.; Adema, G. J.; Boltje, T. J. Sialic acid glycoengineering using an unnatural sialic acid for the detection of sialoglycan biosynthesis defects and on-cell synthesis of siglec ligands. *ACS Chem. Biol.* **2015**, *10*, 2353–2363.
- (27) Bai, X.; Brown, J. R.; Varki, A.; Esko, J. D. Enhanced 3-O-sulfation of galactose in Asn-linked glycans and Maackia amurensis lectin binding in a new Chinese hamster ovary cell line. *Glycobiology* **2001**, *11*, 621–632.
- (28) Malaprade, L. A study of the action of polyalcohols on periodic acid and alkaline periodates. *Bull. Soc. Chim. Fr.* **1934**, *5*, 833–852.

(29) Moons, S. J.; Rossing, E.; Heming, J. J.; Janssen, M. A.; van Scherpenzeel, M.; Lefeber, D. J.; de Jonge, M. I.; Langereis, J. D.; Boltje, T. J. Structure–Activity Relationship of Fluorinated Sialic Acid Inhibitors for Bacterial Sialylation. *Bioconjugate Chem.* **2021**, *32*, 1047.

(30) Burkart, M. D.; Zhang, Z.; Hung, S.-C.; Wong, C.-H. A new method for the synthesis of fluoro-carbohydrates and glycosides using selectfluor. *J. Am. Chem. Soc.* **1997**, *119*, 11743–11746.

(31) von Itzstein, M.; Jin, B.; Wu, W.-Y.; Chandler, M. A convenient method for the introduction of nitrogen and sulfur at C-4 on a sialic acid analogue. *Carbohydr. Res.* **1993**, *244*, 181–185.

(32) Ariza, X.; Urpí, F.; Vilarrasa, J. A practical procedure for the preparation of carbamates from azides. *Tetrahedron Lett.* **1999**, *40*, 7515–7517.